

# Density matrix renormalization calculations of the relaxed energies and solitonic structures of polydiacetylene

Alan Race,<sup>1</sup> William Barford,<sup>1,\*</sup> and Robert J. Bursill<sup>2,†</sup>

<sup>1</sup>*Department of Physics and Astronomy, The University of Sheffield, Sheffield, S3 7RH, United Kingdom*

<sup>2</sup>*School of Physics, The University of New South Wales, Sydney, NSW 2052, Australia*

(Received 6 February 2003; published 12 June 2003)

The density matrix renormalization group method is applied to the Pariser-Parr-Pople-Peierls model to calculate the energies and associated structures of the low-lying states of polydiacetylene. The extrinsic dimerization of polydiacetylene, arising from the electrons in  $p_y$  orbitals in the triple bonds, is explicitly calculated. We find the following results. (i) Electronic interactions result in a twofold increase in the ground state dimerization, and a twofold decrease in the electronic correlation length,  $\xi$ . (ii) The vertical energy of the  $2^1A_g^+$  state lies circa. 1 eV above the  $1^1B_u^-$  state in long chains. (iii) The  $1^3B_u^+$  and  $2^1A_g^+$  states undergo a sizable electron-lattice relaxation, while this is modest for the  $1^1B_u^-$  state. As a consequence, the relaxed energy of the  $2^1A_g^+$  lies circa 0.1 eV below the relaxed energy of the  $1^1B_u^-$  state. (iv) The reduction in  $\xi$  results in a reversal in bond dimerizations in both the  $1^3B_u^+$  and  $2^1A_g^+$  states (in contrast to the noninteracting Peierls model). However, the excitonic  $1^1B_u^-$  state shows a polaronic distortion. We compare our results to experiment. For short oligomers the comparisons are very reasonable, but they are less satisfactory for long chains. The inclusion of solvation effects and a reparametrization of the Ohno interaction may both be necessary.

DOI: 10.1103/PhysRevB.67.245202

PACS number(s): 71.10.Fd, 71.20.Rv, 71.35.Aa

## I. INTRODUCTION

There are a number of reasons why a computational and theoretical study of the electronic states of polydiacetylene (PDA),  $(C_4R_2)_x$  [where R is hydrogen or an alkyl group], is both interesting and instructive. First, in common with all one-dimensional conjugated polymers, polydiacetylene exhibits a wealth of different kinds of excitations. These include magnons, bound magnons, and excitons. These excitations are further enriched by their coupling to the lattice. Second, the relative energetic ordering of these excitations determines the optical properties of the polymer. So, developing an understanding of the reasons for this ordering is an important predictive tool. Finally, polydiacetylene is probably the best experimentally characterized polymer, so it is a good system with which to test the predictions of theory.

Until recently, understanding the combined effects of electron-electron interactions and electron-lattice coupling had been an almost impossible task. However, with the advent of the density matrix renormalization group (DMRG) (Ref. 1) method realistic models of  $\pi$ -conjugated polymers can now be solved, and greater insight is being obtained as to the nature of the low-lying excitations. The Pariser-Parr-Pople-Peierls (PPPP) model is such a realistic model of  $\pi$ -conjugated systems: it is a tight-binding model of the  $\pi$ -electrons, including both long-range  $1/r$  interactions and electron-lattice coupling. The DMRG method has recently been applied to the PPPP model of linear polyenes, and the excited states and associated solitonic structures were investigated.<sup>2,3</sup> In this paper we present our investigations of the same model applied to polydiacetylene.

In the polyene calculations we found that the  $2^1A_g^+$  state is so strongly coupled to the lattice that its relaxed energy lies circa 1 eV below the relaxed energy of the  $1^1B_u^-$  state. (Indeed, there is an energy reversal, as the vertical energy of

the  $2^1A_g^+$  state lies just above the  $1^1B_u^-$  state.) This result agrees with the widely held observation that trans-(CH)<sub>x</sub> is not electroluminescent. The question as to whether there is a sub-band  $A_g$  state in polydiacetylene is more equivocal, with many authors arguing that there is such as state.<sup>4,5</sup>

In an earlier paper,<sup>6</sup> the current authors used the Pariser-Parr-Pople model to study the vertical excitations energy of polydiacetylene. The Pariser-Parr-Pople model was parametrized from earlier studies of conjugated oligomers, and using the polydiacetylene bond lengths from Giesa and Schultz.<sup>7</sup> The electron-phonon coupling constant  $\alpha$ , used to derive the hybridization integrals, was obtained from our studies of trans-(CH)<sub>x</sub>.<sup>3</sup> We obtained good agreement with the experimental results of Giesa and Schultz<sup>7</sup> for the  $1^1B_u^-$  energies of oligomers in hexane solution (with the side groups,  $R=H$ ). Our long-chain prediction of circa 3.0 eV for the  $1^1B_u^-$  energy is in reasonable agreement with the extrapolated experimental oligomer energy of circa 2.5 eV. However, our prediction lies over 1 eV higher in energy than the results of Weiser and co-workers, who find the  $1^1B_u^-$  energy at circa 1.9 eV in crystalline polydiacetylene.<sup>8,9</sup> These discrepancies indicate that the Pariser-Parr-Pople model may not be so well parametrized for long chain polymers in the solid state. We also found that the vertical energy of the  $2^1A_g^+$  state lies circa 1.0 eV higher than the  $1^1B_u^-$  energy.

In this work, we use the results of the Pariser-Parr-Pople calculations<sup>6</sup> to parametrize the additional parameter in the PPPP model, namely the dimensionless electron-phonon coupling parameter  $\lambda$ . The stereochemistry of polydiacetylene is different from that of linear polyenes is one crucial aspect, namely, the  $sp$  hybridization of the triple bonds results in an extrinsic dimerization.<sup>10</sup> Thus, undoped polydiacetylene is semi-conducting, irrespective of the ground state broken symmetries driven by the  $\pi$  electrons. This has a number of

important consequences for the effects of the intrinsic dimerization. First, since the ground state is no longer degenerate, there is a linear confining potential between the soliton and antisoliton. Second, there are four midgap states (rather than just two, as in linear polyenes.) This means that the  $2^1A_g^+$  state consists of four solitons, not just two. The extrinsic dimerization also affects the excitation energies determined by the  $\pi$ -electron interactions. In a uniform chain, as for the linear polyenes with  $\lambda=0$ , the lowest spin-density-wave states, namely the  $1^3B_u^+$  triplet and the  $2^1A_g^+$  state are gapless, while the excitonic  $1^1B_u^-$  state is not. For a chain with extrinsic dimerization, however, all the excitations are gapped, and for sufficiently large dimerization the  $2^1A_g^+$  state will lie above the  $1^1B_u^-$  state.

To understand the rôles of electron-electron interactions and electron-lattice coupling in determining the characteristics and energies of the excited states, we study the PPPP model in the limiting cases of nonzero  $U$ , zero  $\lambda$  (the Pariser-Parr-Pople model) and zero  $U$ , nonzero  $\lambda$  (the Peierls model), before the general case of nonzero  $U$ , nonzero  $\lambda$  is considered. Before that, however, we parametrize the PPPP model for polydiacetylene by determining the extrinsic dimerization arising from the triple bonds.

## II. PARISER-PARR-POPLE-PEIERLS HAMILTONIAN

We are principally interested with the low-energy electronic structure and associated geometries arising from the delocalized  $\pi$  electrons. Before considering this, however, we need to understand the rôles of the  $\sigma$  and  $p_y$  electrons. Each unit cell consists of two  $sp^2$  hybridized carbon atoms and two  $sp$  hybridized carbon atoms. The electrons in the  $\sigma$  orbitals are responsible for the overall structural integrity of the molecule, and for the in-plane bond angles. The electrons in the  $p_y$  orbitals do not delocalize, but they cause the ‘‘triple’’ bond to shorten. The  $\pi$  (or  $p_z$ ) electrons delocalize throughout the molecule, cause the overall chain length to shorten, and lead to a ‘‘dimerized’’ chain, whereby some bonds shorten and others lengthen. We denote the chain structure before dimerization by the  $\pi$  electrons as the unrelaxed, or undistorted geometry. We denote the chain structure after dimerization as the relaxed, or distorted geometry. With these definitions the overall chain length of the distorted chain equals that of the undistorted chain. Figure 1 shows the undistorted and distorted geometries.

We represent the inequivalent bonds prior to distortion by the  $\pi$ -electrons by the different bond hybridization integrals:

$$\bar{t}_l \text{ and } \bar{r}_l = \begin{cases} t_1 \text{ and } r_1: & \text{bonds including } p_y \text{ orbitals} \\ t_2 \text{ and } r_2: & \text{otherwise} \end{cases} \quad (1)$$

We denote the dimerization caused by the  $\pi$ -electrons as the intrinsic dimerization,  $\Delta_l^i$ . Similarly, we denote the effective dimerization caused by the  $p_y$  electrons as the extrinsic dimerization  $\Delta_l^e$ .

The Pariser-Parr-Pople-Peierls model for the  $\pi$  electrons is defined as

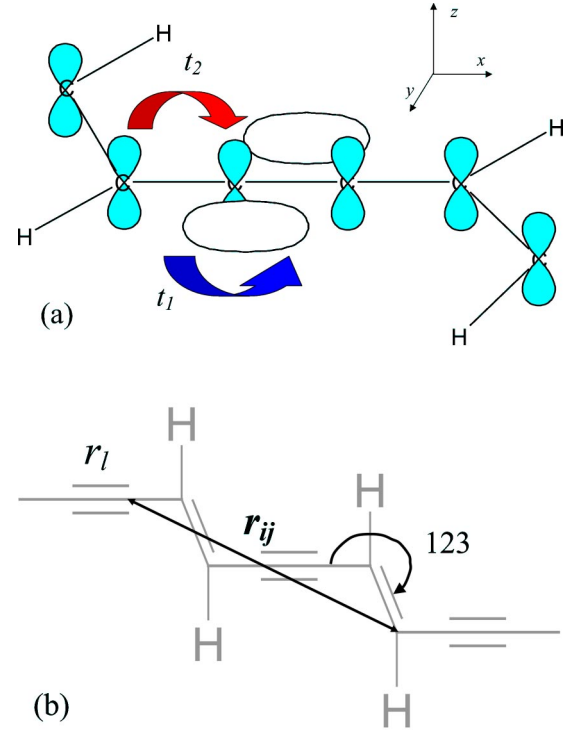


FIG. 1. The parametrization of the Pariser-Parr-Pople-Peierls Hamiltonian for polydiacetylene. (a) A schematic diagram of the  $\sigma$ - $p_y$  backbone before the lattice has been dimerized by the  $\pi$ -electrons.  $t_1$  is the hybridization integral for the ‘‘triple’’ bond (containing both  $p_y$  and  $p_z$  orbitals) before dimerization by the  $\pi$  orbitals.  $t_2$  is the hybridization integral for the other bonds. (b) The geometry of the polydiacetylene chain.

$$\hat{H} = -2 \sum_{l=1}^{N-1} t_l \hat{T}_l + \frac{1}{4\pi t_0 \lambda} \sum_{l=1}^{N-1} (\Delta_l^i)^2 + U \sum_{i=1}^N \left( \hat{n}_{i\uparrow} - \frac{1}{2} \right) \times \left( \hat{n}_{i\downarrow} - \frac{1}{2} \right) + \sum_{\langle ij \rangle} V_{ij} (n_i - 1)(n_j - 1), \quad (2)$$

where  $\langle \rangle$  indicates all pairs of sites,

$$t_l = (\bar{t}_l + \Delta_l^i/2), \quad (3)$$

and  $\bar{t}_l$  is the undistorted hybridization integral given by Eq. (1).

$$\hat{T}_l = \frac{1}{2} \sum_{\sigma} (c_{l+1\sigma}^\dagger c_{l\sigma} + \text{H.c.}) \quad (4)$$

is the bond order operator of the  $l$ th bond.  $V_{ij}$  is the Ohno potential, defined by

$$V_{ij} = \frac{U}{\sqrt{1 + (U r_{ij}/14.397)^2}}, \quad (5)$$

with the bond lengths in Å. The dimensionless electron-phonon coupling constant  $\lambda$  is defined by

$$\lambda = \frac{2\alpha^2}{\pi K t_0}, \quad (6)$$

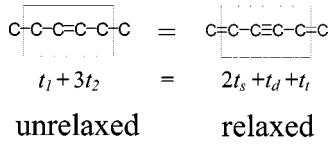


FIG. 2. The hybridization integrals in polydiacetylene. The hybridization integrals in a unit cell of the unrelaxed chain equal the hybridization integrals for a relaxed chain. We used the bond lengths determined by the x-ray structure analysis of Giesa and Schultz (Ref. 7) to generate the ground state hybridization integrals  $t_s$ ,  $t_d$  and  $t_t$  (Ref. 6).  $t_1$  and  $t_2$  are described in Fig. 1(a).

where  $K$  is the elastic spring constant (estimated to be  $46 \text{ eV } \text{\AA}^{-2}$  for C-C bonds<sup>12</sup>).  $\alpha$  relates  $\delta r_l$ , the change in bond length of the  $l$ th bond from its undistorted value ( $\bar{r}_l$ ), to  $\Delta_l^i$  as

$$\delta r_l = -\Delta_l^i / 2\alpha. \quad (7)$$

$t_0$  is taken to be the hybridization integral of a C-C bond of  $1.4 \text{ \AA}$ , namely,  $2.539 \text{ eV}$ . Finally,  $\Gamma$  is determined self-consistently to enforce constant chain lengths:

$$\sum_{i=1}^{N-1} \Delta_i^i = 0. \quad (8)$$

The relaxed geometry is determined when the force per bond  $f_l$  vanishes. Using the Hellmann-Feynman theorem  $f_l$  can be expressed as

$$\begin{aligned}
 f_l = & -2\alpha \left( \frac{\Delta_l^i}{2\pi t_0 \lambda} + \Gamma - \langle \hat{T}_l \rangle \right) - \sum_{\langle ij \rangle} \frac{\beta U}{(1 + \beta r_{ij}^2)^{3/2}} \\
 & \times \left( x_{ij} \frac{\partial x_{ij}}{\partial \Delta_l^i} + y_{ij} \frac{\partial y_{ij}}{\partial \Delta_l^i} \right) \langle (\hat{n}_i - 1)(\hat{n}_j - 1) \rangle. \quad (9)
 \end{aligned}$$

We take polydiacetylene to have constant bond angles. This is borne out in experiments where the bond angles are seen to remain approximately constant for a wide range of polymer lengths and functional groups.<sup>7</sup> An illustration of polydiacetylene, with its constant bond angles, is shown in Fig. 1(b). For constant bond angles,  $x_l$  and  $y_l$  are defined as

$$x_l = r_l \cos(180^\circ - 123^\circ) = \left( \bar{r} - \frac{\Delta_l^i}{2\alpha} \right) \cos(57^\circ)$$

for the bonds at an angle of  $123^\circ$  from the  $x$  axis, or

$$x_l = \bar{r} - \frac{\Delta_l^i}{2\alpha} \quad (10)$$

otherwise. Similarly,

$$y_l = - \left( \bar{r} - \frac{\Delta_l^i}{2\alpha} \right) \sin(57^\circ) \quad (11)$$

for the bonds at an angle of  $123^\circ$  from the  $x$  axis, or

$$y_l = 0 \quad (12)$$

TABLE I. The optimal parameters used in the Pariser-Parr-Pople-Peierls Hamiltonian applied to polydiacetylene.

Parameter	Value
$r_1$	$1.285 \text{ \AA}$
$r_2$	$1.400 \text{ \AA}$
$t_1$	$2.687 \text{ eV}$
$t_2$	$3.067 \text{ eV}$
$\lambda$	$0.085$
$\alpha$	$4.062 \text{ eV } \text{\AA}^{-1}$
$\tilde{K}_{eff} \sim K$	$46 \text{ eV } \text{\AA}^{-2}$

otherwise.

Setting  $f_l = 0 \forall l$  yields a self-consistent equation for the equilibrium  $\Delta_l^i$ , which is solved using the fixed-point iteration method, with an initial guess  $\Delta_l^i = 0 \forall l$ . We use the infinite-lattice DMRG method, so as to enforce  $\hat{C}_2$  symmetry. The calculation of the relaxed energy of a given state for a given chain length is as follows.

(1) The eigenstate is calculated for an initial choice of  $\{\Delta_{ij}^i\}$  by building up the lattice to the target chain size using the infinite lattice algorithm of the DMRG method.

(2) At the target chain size the condition  $f_l = 0$  is repeatedly applied until the  $\{\Delta_{ij}^i\}$  have converged.

(3) Using the new values of  $\{\Delta_{ij}^i\}$ , steps (1) and (2) are repeated. The procedure is successfully terminated when the energies have converged after successive Hellmann-Feynman iterations.

### A. Parametrization of the Hamiltonian

The undistorted hybridization integrals  $t_1$  and  $t_2$  are determined by the extrinsic dimerization of the ‘triple’ bond (caused by the  $p_y$  electrons), subject to the constraint that

$$t_1 + 3t_2 = 2t_s + t_d + t_t = \text{const}, \quad (13)$$

where  $t_s$ ,  $t_d$ , and  $t_t$  are the single, double, and triple bond hybridization integrals used in Ref. 6 (see Fig. 2). The electrons in the  $p_y$  orbitals on each ‘triple’ bond are also subject to a Pariser-Parr-Pople-Peierls model, where  $\Delta_l^i$  is replaced by  $\Delta^e$ . We take  $\lambda$  to be the free parameter that determines the values of  $t_1$  and  $t_2$ , subject to Eq. (13).

The  $p_y$  orbitals are expected to act independently of the bulk of the system and mix very little in character with other orbitals, thereby acting as a two site system. If we take a pair of  $p_y$  orbitals in isolation and set the bond force—obtained by the Hellmann-Feynman condition—to zero, we obtain a self-consistent equation for  $\Delta^e$ , given by Eq. (A10) in the Appendix. As the underlying physics of the two-site system is expected to be the same as that of a double bond in polyacetylene, the values of  $t_0$ ,  $U$  and  $r_0$  used in Eq. (A10) are the values used in the C-C bonds of polyacetylene (namely,  $t_0 = 2.539 \text{ eV}$ ,  $r_0 = 1.4 \text{ \AA}$ , and  $U = 10.06 \text{ eV}$ ).

For various values of  $\lambda$ , we generated values of  $t_1$  and  $t_2$ , by solving Eq. (A10) to find the hybridization integral  $t_1$ , and using Eq. (13) to find  $t_2$ . Various ground state, relaxed

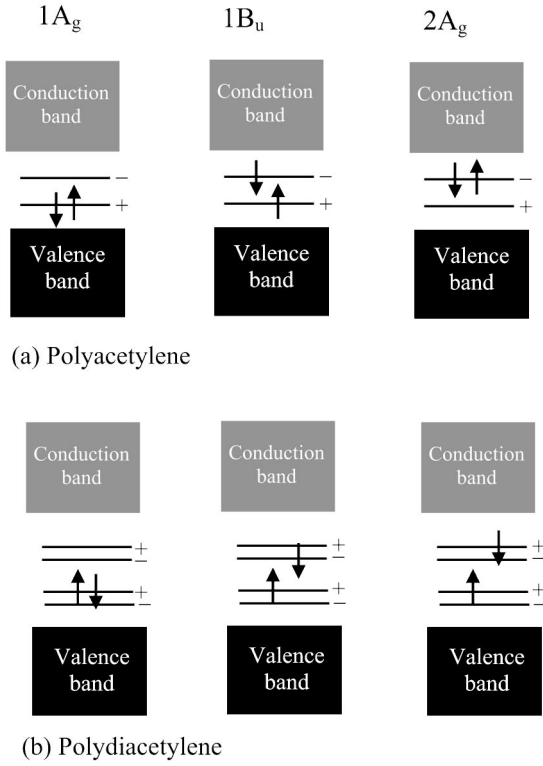


FIG. 3. A comparison between the occupied molecular orbitals in the Peierls model for polyacetylene and polydiacetylene. In polyacetylene the  $2A_g$  state is obtained by promoting two electrons from the highest occupied (HOMO) to lowest unoccupied molecular orbital (LUMO). However, in polydiacetylene, it is obtained by promoting one electron from the HOMO to the LUMO + 1 (or the HOMO - 1 to the LUMO).

long-chain geometries were then calculated by performing the Hellman-Feynman routine on the Pariser-Parr-Pople-Peierls Hamiltonian of the  $\pi$  electrons [Eq. (2)], for each parameter set. These geometries were then used to fit the vertical energies of the Pariser-Parr-Pople-Peierls model to the vertical energies of the Pariser-Parr-Pople model presented in Ref. 6, the best fit giving the optimal set of parameters  $\{\lambda, t_1, t_2\}$ . These optimal parameters are shown in Table I. A choice of  $\lambda = 0.085$  gives a long-chain vertical energies of 3.104 and 3.862 eV, compared with the values of 3.102 and 3.862 eV from the Pariser-Parr-Pople-Peierls model, for the  $1^1B_u^-$  and  $2^1A_g^+$  states, respectively. This suggests the Hamiltonian is accurately parametrized.<sup>11</sup>

Finally, as we have already mentioned, an electron in the bond  $t_1$  experiences a different potential to an electron in bond  $t_2$ ; hence, on first inspection one would think the spring constant of bond  $t_1$  different from that of  $t_2$ . We found the new effective spring constant  $\tilde{K}_{eff}$  from

$$\tilde{K}_{eff} = - \frac{\partial^2 V(\Delta^e)}{\partial^2 \Delta^e} \langle (\hat{n}_1 - 1)(\hat{n}_2 - 1) \rangle + K |_{\lambda=0.085}. \quad (14)$$

Evaluating the first term on the right-hand-side of Eq. (14), including the Coulomb correlator, gives

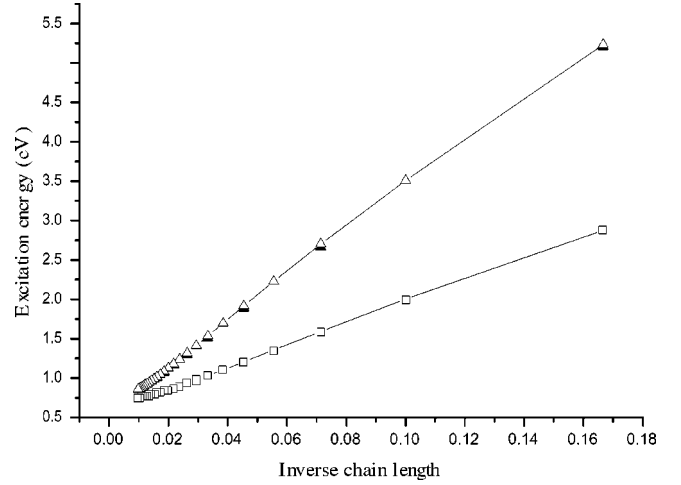


FIG. 4. A comparison between the DMRG (full symbols) and exact (open symbols) calculations of the Peierls ( $U=0$  and  $\lambda \neq 0$ ) model of the  $1^1B_u^-$  (squares) and  $2^1A_g^+$  (triangles) excitation energies.

$$\tilde{K}_{eff} = K - 0.02 \text{ eV } \text{\AA}^{-2} \sim K. \quad (15)$$

Hence, the new spring constant is essentially the same as the value derived from the Raman analysis of the C-C stretching modes in trans-(CH)<sub>x</sub> (see Table I).<sup>12</sup>

### III. PEIERLS MODEL

Setting  $U=0$  in the P-P-P-P model defines the Peierls model. Figure 3 shows a schematic energy diagram of the molecular orbitals and defect states for polyacetylene and polydiacetylene within this model. In polyacetylene there are two midgap states. In contrast, the extrinsic dimerization present in polydiacetylene results in four midgap states. The  $2^1A_g^+$  state in polyacetylene is formed by the double occupancy of the antibonding molecular orbital. However, in polydiacetylene the  $2^1A_g^+$  state is formed by exciting a *single* electron into a higher-lying molecular orbital, and consequently there are four associated geometrical defects (or solitons).

Since the non-interacting Peierls model can be solved exactly for a given bond order, we use this model to validate the DMRG method. A graph of the exact and DMRG-calculated excitation energies for the  $2^1A_g^+$  and  $1^1B_u^-$  states are shown in Fig. 4, indicating excellent agreement. The  $2^1A_g^+$  state lies energetically above the  $1^1B_u^-$  state, as expected. However, in the thermodynamic limit these states become degenerate, with an excitation energy  $\sim 0.066$  eV.

The associated relaxed geometries generated by the two calculations are presented in Fig. 5. In this plot we introduce the normalized, staggered bond dimerization for the  $l$ th bond as

$$\delta_l = (-1)^l \frac{(t_l - \bar{t})}{\bar{t}}. \quad (16)$$

The geometries are in excellent quantitative agreement. We note the lack of a bond reversal for any state, as the soliton

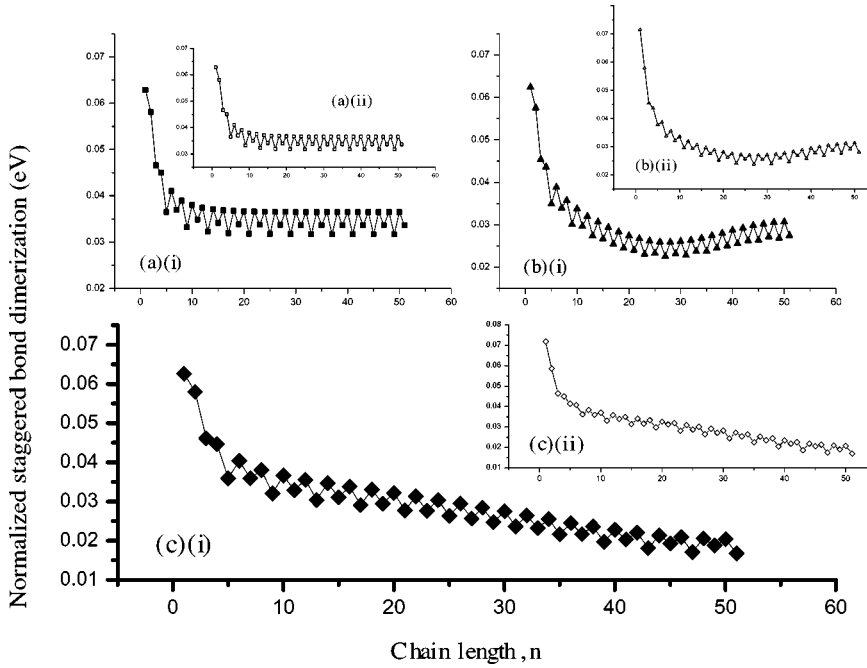


FIG. 5. Comparisons between the DMRG and exact calculations of the Peierls ( $U=0$  and  $\lambda \neq 0$ ) model of the normalized, staggered bond dimerization,  $\delta_l$ . The graphs shows half a polymer, and can be reflected at  $N=51$  to give the full polymer. (a)  $1^1A_g^+$  state (i) exact (ii) DMRG; (b)  $2^1A_g^+$  state (i) exact (ii) DMRG; (c)  $1^1B_u^-$  state (i) exact (ii) DMRG. Note that because of the extrinsic dimerization, there is no bond reversal for any state.

and antisoliton experience a linear confining potential as a result of the extrinsic dimerization. Further, as already discussed, the  $2^1A_g^+$  state shows a tightly-bound four soliton fit, while the  $1B_u^-$  state shows a tightly-bound two soliton fit. These states are composite quasiparticles, and they exhibit polaronlike dimerization patterns with weak lattice distortions.<sup>13</sup> These results help us understand the role of electronic interactions in the solitonic structure of the excited states, as we shall discuss in more detail in Sec. V D.

#### IV. SOLUTION OF THE PARISER-PARR-POPPE MODEL

The spin excitations are gapless in the thermodynamic limit of a uniform chain at half filling with only on-site electron-electron interactions. This result remains true for long-range interactions.<sup>3</sup> In contrast, in the  $\lambda=0$  limit of the P-P-P model (i.e., the Pariser-Parr-Pople model), polydiacetylene does not have a uniform lattice, owing to the extrinsic dimerization. As a consequence, the  $1^3B_u^+$  and  $2^1A_g^+$  states are gapped. Figure 6 compares the results of the Peierls model with those of the Pariser-Parr-Pople model. For long-chains  $E(2^1A_g^+) \sim 1.75$  eV, whereas  $E(1^1B_u^-) \sim 1.79$  eV. Hence the energetic ordering is in agreement with most experiments with  $\lambda=0$ .

#### V. SOLUTION OF THE PARISER-PARR-POPPE-PEIERLS MODEL

##### A. Ground state structure and energy profile

The relaxed geometry of the ground state, with the optimal set of parameters  $\{\lambda, t_1, t_2\}_{\text{opt}}$ , yields hopping integrals in the middle of the chain  $t_l$ ,  $t_d$ , and  $t_s$  that are in excellent agreement with the experimentally determined ones found in Ref. 6. Table II compares the hopping integrals. Hence, our first result is that the full solution of the Pariser-Parr-Pople-Peierls model generates a good ground state geometry.

This ground state stability can be explained and explored further by considering how the total ground state energy varies as a function of the dimerization. The calculated values of  $\{t_j\}$  imply that the dimerization of the ground state in the middle of the 102-site chain is  $\Delta^i \sim 0.225 \pm 0.001$  eV. This is the average dimerization, and because the variance from the average is small (0.4%) and gets smaller for longer chains, we can conclude that the  $\pi$  system would be homogeneously dimerized in the thermodynamic limit, tending towards 0.225 eV. Therefore, in the ground state

$$\Delta_l^i = (-1)^{l+1} 0.225 \text{ eV}, \quad (17)$$

implying that  $\delta r_l^i = (-1)^l 0.028 \text{ \AA}$ .

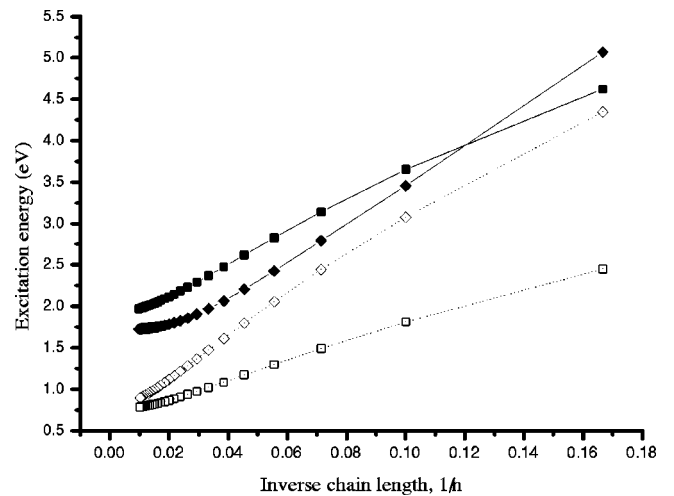


FIG. 6. The effects of Coulomb interactions and electron-phonon interactions on the excitation energies.  $2^1A_g^+$  state (diamonds) and  $1^1B_u^-$  state (squares). The Peierls model ( $U=0$  and  $\lambda \neq 0$ ): open symbols. The Pariser-Parr-Pople model ( $U \neq 0$  and  $\lambda = 0$ ): solid symbols.

TABLE II. A comparison of the hybridization integrals generated by the relaxed geometry calculation of the ground state of polydiacetylene using the Pariser-Parr-Pople-Peierls Hamiltonian with those found from the experimentally-determined bond lengths used in the Pariser-Parr-Pople model (Ref. 6). These are denoted  $t_{\text{PPPP}}$  and  $t_{\text{expt}}$ , respectively.

	$t_{\text{PPPP}}$ (eV)	$t_{\text{expt}}$ (eV)
Triple $t_t$	3.316	3.435
Single $t_s$	2.467	2.449
Double $t_d$	2.891	2.794

The total ground state energy,  $E_{\text{tot}}$ , is given by the  $\pi$ -electron energy  $E_{\pi}$  and the elastic energy  $E_{\sigma,p_y}$ , as

$$E_{\text{tot}} = E_{\pi}(\Delta_l^i, \Delta_l^e) + E_{\sigma,p_y}(\Delta_l^i). \quad (18)$$

Hence, by imposing the homogeneous intrinsic dimerization,

$$\Delta_l^i = (-1)^l \Delta_0^i, \quad (19)$$

we can study how the ground state energy varies as a function of  $\Delta_0^i$ .

The  $\pi$ -electron energy, elastic energy and the total energy are shown in Fig. 7. The total energy shows only one minimum at  $\Delta_0^i \sim -0.22$  eV in the acetylene phase space, in good agreement with the average quoted above. We now roughly estimate the energy difference between acetylene and butatriene structure for 102 sites. For the butatriene structure, we reverse the dimerization (see Fig. 8). The energy difference between the total energies of both structures is therefore

$$\Delta E_{\text{tot}} = E_{\text{tot}}(\Delta_0^i = -0.22) - E_{\text{tot}}(\Delta_0^i = 0.22) = 12.65 \text{ eV}. \quad (20)$$

Thus, per unit cell we have  $\Delta E_{\text{tot}} = 0.495$  eV. This is in very good agreement with the values quoted in the literature of  $\sim 0.5$  eV.<sup>14,15</sup> It is this energy difference that gives the linear

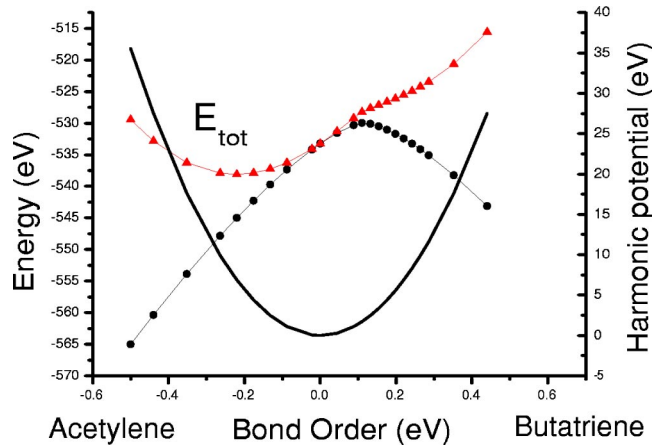


FIG. 7. The ground state energies as a function of the intrinsic bond alternation parameter,  $\Delta^i$ , for a polydiacetylene chain of 102 sites. The total energy of the  $\pi$ -electrons is denoted by circles. The elastic strain energy of the  $\sigma$ - $p_y$  backbone is denoted by the solid curve. The sum of both energies,  $E_{\text{tot}}$ , is denoted by triangles.

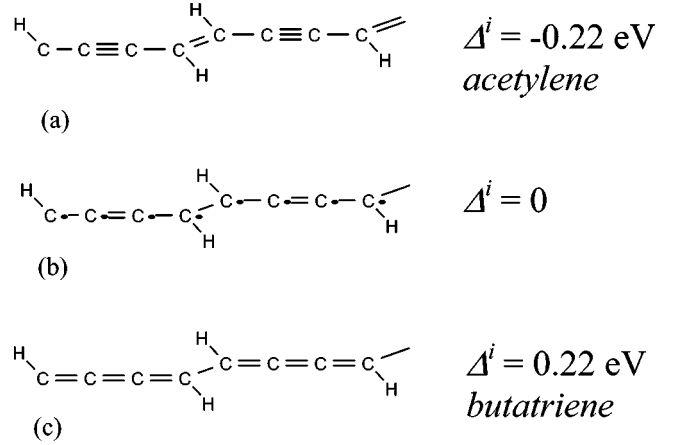


FIG. 8. The structures and their possible dimerization for polydiacetylene. (a) Acetylene structure with  $\Delta^i = -0.22$  eV. (b) Unrelaxed geometry with  $\Delta^i = 0$  eV. (c) Butatriene structure with  $\Delta^i = 0.22$  eV.

confining potential between the soliton and antisoliton, as a bond reversal costs 0.5 eV per unit cell.

### B. Calculated relaxed excited state energies

The vertical energies ( $E^v$ ) of the  $1^3B_u^+$ ,  $1^1B_u^-$  and  $2^1A_g^+$  states are calculated using the ground state geometry. These, and their respective relaxed energies ( $E^{(0-0)}$ ), are shown in Fig. 9 as a function of inverse chain length, and quoted in Table III for 102 sites. We first note that the vertical energies of the  $1^1B_u^-$  and  $2^1A_g^+$  states are circa 1 eV apart; in the thermodynamic limit  $E^v(1^1B_u^-) < E^v(2^1A_g^+)$ .

The relaxation energy of the  $1^1B_u^-$  state is modest ( $\sim 0.14$  eV) for 102 sites. Conversely, the relaxation energies of the  $1^3B_u^+$  and  $2^1A_g^+$  states are substantial, being  $\sim 0.5$  and 1.0 eV, respectively, converging rapidly with  $N$ . The large  $2^1A_g^+$  and  $1^3B_u^+$  relaxation energies are a consequence of the large distortion away from the ground state structure. The graph in the inset of Fig. 9 shows the difference between  $E^{(0-0)}(1^1B_u^-)$  and  $E^{(0-0)}(2^1A_g^+)$ . These values are tending towards a long chain value of  $\sim 0.1$  eV.

The charge gap is also shown in Fig. 9. In the thermodynamic limit the charge gap represents the energy of an uncorrelated electron-hole pair. As expected, the charge gap relaxation energy ( $\sim 0.3$  eV) is about twice that of the  $1^1B_u^-$  state ( $\sim 0.14$  eV), as the free charges form polarons, whereas the  $1^1B_u^-$  state forms a single, bound exciton polaron. The single chain exciton binding energy is predicted to be 2.6 eV.

For long chains, the  $2^1A_g^+$  and  $1^3B_u^+$  states show deviations from the  $1/N$  behavior; however, the  $1^1B_u^-$  state and the polaron do not. In the Pariser-Parr-Pople-Peierls model states that form pronounced solitonic structures self-trap once the chain length exceeds their spatial extent.<sup>17</sup> As we shall see in Sec. V C, the  $2^1A_g^+$  and  $1^3B_u^+$  states have localized solitonic dimerizations, which corroborates this idea. Calculations on polyacetylene have shown similar results.<sup>3</sup>

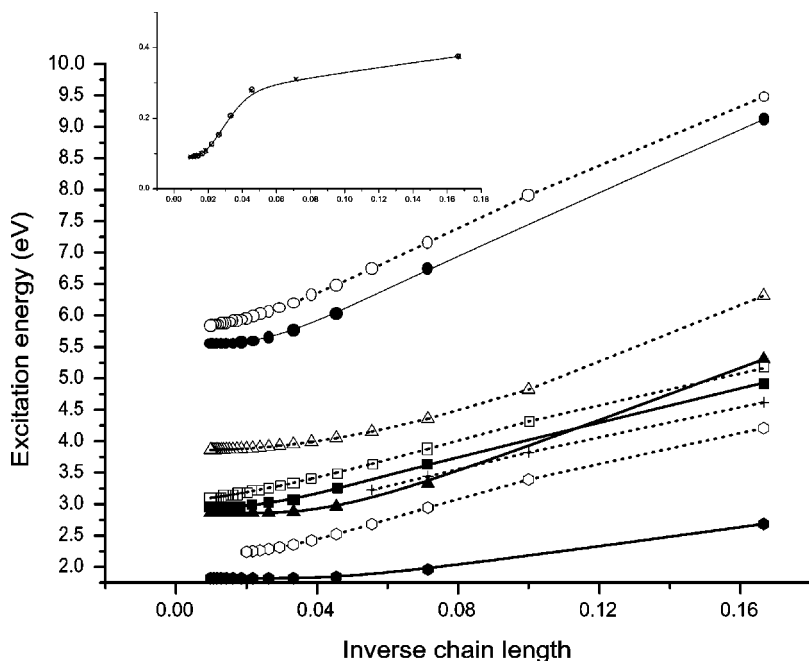


FIG. 9. The excitation energies for the  $1^1B_u^-$  (squares),  $1^3B_u^-$  (hexagons), and  $2^1A_g^+$  (triangles) states, and the charge gap (circles) as a function of the inverse number of carbon atoms. Vertical and relaxed transitions are indicated by dashed and solid lines and open and solid symbols, respectively. The experimental vertical transitions of the  $1^1B_u^-$  state (crosses) are also shown (Ref. 7). The inset shows  $|E^{(0-0)}(1^1B_u^-) - E^{(0-0)}(2^1A_g^+)|$ .

### C. Comparison to experimental energies

Our calculated energies for short oligomers are in very reasonable agreement with experiment. Figure 9 shows the experimental vertical  $1^1B_u^-$  energies.<sup>7</sup> Kohler and Schilke<sup>4</sup> have also observed a vertical absorption of 3.22 eV and a vertical emission at 2.79 eV in butyl-capped  $C_2(C_4H_2)_3$ . They also observed a two-photon feature at 3.04 eV. Subgap two-photon signals have also been observed by Townsend and co-workers.<sup>5</sup> Our relaxed triplet energy of 1.8 eV agrees well with the observation of phosphorescence from triplets at 1.72 eV by Winter *et al.*<sup>16</sup> However, as already discussed in the Introduction, our long chain predictions for the  $1^1B_u^-$  energies disagree by circa 1 eV from Wieser's and co-workers' observations on crystalline PDA.<sup>8</sup> Similarly, our predicted binding energies are considerably larger than the single crystalline results of circa 0.5 eV, observed by both Franz-Keyldish oscillations<sup>8</sup> and photoconductivity.<sup>9</sup> While some of this discrepancy can be attributed to solvation effects,<sup>18</sup> not modeled by a single chain PPPP calculation, it does seem likely that a re-parametrization of the Ohno interaction is necessary for long chains in a crystalline environment.<sup>19</sup> In conclusion, as the PPPP model is not accurate to 0.1 eV, our calculation that the relaxed  $2^1A_g^+$  energy lies below the relaxed  $1^1B_u^-$  energy may not be true for all PDA polymers in all environments.

TABLE III. Energies for various states of polydiacetylene with 102 sites.

State	$E_{102}^{(v)}$	$E_{102}^{(0-0)}$
$1^1B_u^-$	3.10	2.95
$2^1A_g^+$	3.86	2.86
$1^3B_u^+$	2.90	1.82
charge-gap	5.85	5.55

### D. Solitonic structures

In Fig. 10 we plot the normalized, staggered bond dimerization  $\delta_l$  for the PPPP model. This illustrates how electronic interactions affect the electronic states. By comparing to the bond distortions of the Peierls model (Fig. 5), we see that interactions roughly double the dimerization in the ground state of the Peierls model. This increase is expected.<sup>20,21</sup>

The  $1^1B_u^-$  state is polaronic in form, in both the Peierls and Pariser-Parr-Pople-Peierls models. However, electronic interactions increase the soliton-antisoliton confinement, as they cause the oppositely charged soliton and antisoliton to bind strongly, forming an exciton-polaron. The exciton-polaron geometry is almost undistinguishable from that of the doped charge.

The two spin 1/2 spinons in the soliton-antisoliton pair of the  $1^3B_u^+$  state do not bind by electronic interactions, but do

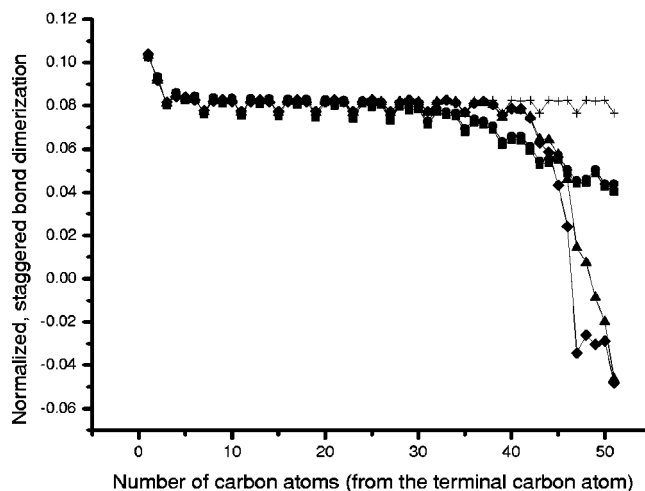


FIG. 10. The dimerization  $\delta_l$ , (from the end of the chain) of the  $1^1A_g^+$  (crosses),  $2^1A_g^+$  (diamonds),  $1^3B_u^+$  (triangles), and  $1^1B_u^-$  (squares) states, and the polaron (circles).

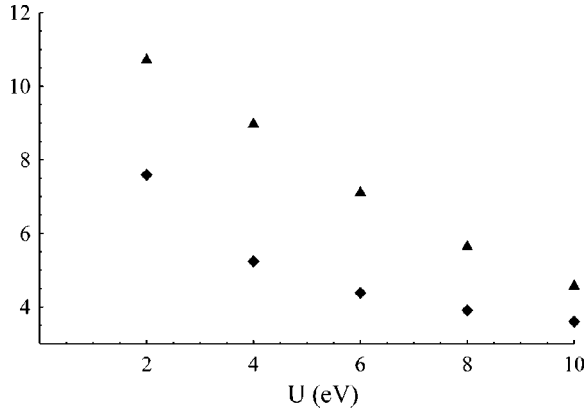


FIG. 11. The soliton width  $\xi$  (triangles) and half the soliton-antisoliton separation,  $x_0$  (diamonds), for the triplet state as a function of  $U$ , obtained by fitting Eq. (21) to the calculated staggered bond dimerization.

bind by the confinement arising from the difference in energy between the acetylene and butatriene structures. Figure 10 shows that there is now a bond reversal for this state in the interacting model. This arises from a reduction in the electronic correlation length,  $\xi \sim a/\delta$ , as shown in the fits of the two-soliton form,

$$\delta_l = \bar{\delta} (1 + \tanh(2x_0/\xi) \{ \tanh[(l-x_0)/\xi] - \tanh[(l-x_0)/\xi] \}), \quad (21)$$

in Fig. 11 as a function of  $U$ . Indeed, the soliton-antisoliton separation,  $2x_0$ , decreases as a function of  $U$ , because the difference in energy between the acetylene and butatriene structures is greater in the interacting model.

As already discussed, even for the Peierls model the  $2^1A_g^+$  state requires a four-soliton fit of the form

$$\delta_l = \bar{\delta} (1 + \tanh(x_0/\xi) \{ \tanh[(l-x_d-x_0)/\xi] - \tanh[(l-x_d+x_0)/\xi] + \tanh[(l+x_d-x_0)/\xi] - \tanh[(l+x_d+x_0)/\xi] \}). \quad (22)$$

In linear polyenes the  $2^1A_g^+$  state has a substantial triplet-triplet character,<sup>22–25</sup> and is thus composed of four solitons. This triplet-triplet character is also present in the  $2^1A_g^+$  state of polydiacetylene, and causes an additional attraction between the soliton-antisoliton pairs. This is illustrated in Fig. 12.

## VI. CONCLUSIONS

The density matrix renormalization group method has been applied to the Pariser-Parr-Pople-Peierls model to calculate the energies and associated structures of the low-lying states of polydiacetylene. The extrinsic dimerization of polydiacetylene—arising from the  $p_y$  orbitals—results in different physical behavior to that of linear polyenes.

For the PPPP model in the  $\lambda=0$  limit (that is, without  $\pi$ -electron dimerization) the excited states are gapped, because of the extrinsic dimerization. For realistic Coulomb

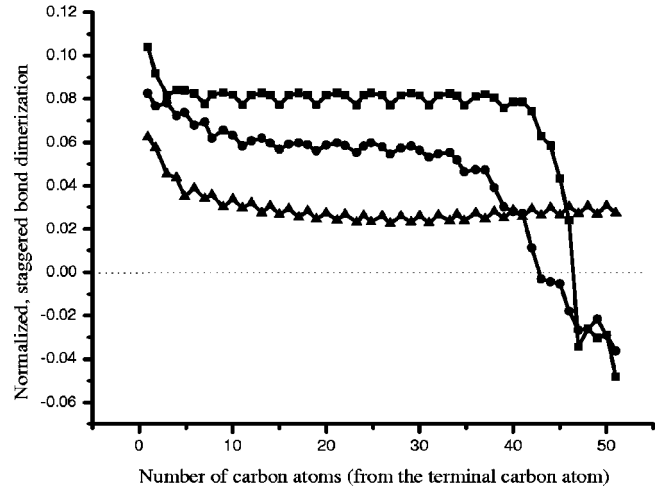


FIG. 12. The evolution of the dimerization,  $\delta_l$ , of the  $2^1A_g^+$  state with increasing  $U$ .  $U=10$  eV (squares),  $U=7$  eV (circles), and  $U=0$  eV (triangles).

interactions the  $2^1A_g^+$  energy lies below the  $1^1B_u^-$  energy. Conversely, for the PPPP model in the  $U=0$  limit the  $2^1A_g^+$  state fits a four-soliton form, as there are four midgap states. The  $1^1B_u^-$  state fits a two-soliton form. The extrinsic dimerization results in a linear confining potential between the soliton and antisoliton, and there is no bond reversal.

When both electronic interactions and electron-lattice coupling are both considered we find the following results. (i) There is a twofold increase in the ground state dimerization, and a twofold decrease in the electronic correlation length,  $\xi = a/\delta$ . (ii) The vertical energy of the  $2^1A_g^+$  state lies circa 1 eV above the  $1^1B_u^-$  state. (iii) The  $1^3B_u^+$  and  $2^1A_g^+$  states undergo a sizable electron-lattice relaxation, while this is modest for the  $1^1B_u^-$  state. As a consequence, the relaxed energy of the  $2^1A_g^+$  lies circa 0.1 eV below the relaxed energy of the  $1^1B_u^-$  state. (iv) The reduction in  $\xi$  results in a reversal in bond dimerizations in both the  $1^3B_u^+$  and  $2^1A_g^+$  states. However, the excitonic  $1^1B_u^-$  state still shows a polaronic distortion.

We compared our results to experiment. For short oligomers the comparisons are very reasonable, but they are less satisfactory for long chains. The inclusion of solvation effects<sup>18</sup> and a reparametrization of the Ohno interaction may both be necessary. However, the prediction of a subgap  $A_g$  state is borne out by most experiments.<sup>4,5</sup>

## ACKNOWLEDGMENTS

This work was supported by the EPSRC (U.K.) (GR/R03921). A.R. was supported by the EPSRC, and R.J.B. is supported by the Australian Research Council and the J G Russell Foundation.

## APPENDIX: THE TREATMENT OF $p_y$ ELECTRONS IN THE TRIPLE BOND

At half filling and in the  $S=0$  subspace, the two-site basis that models the electrons in  $p_y$  orbitals on the triple bond is



$$|1\rangle = \frac{1}{\sqrt{2}}(|\uparrow 0, 0\downarrow\rangle - |0\downarrow, \uparrow 0\rangle),$$

$$|2\rangle = \frac{1}{\sqrt{2}}(|\uparrow\downarrow, 00\rangle + |00, \uparrow\downarrow\rangle). \quad (\text{A1})$$

This generates the Pariser-Parr-Pople Hamiltonian matrix

$$\hat{H} = \begin{pmatrix} V(\Delta^e) & -2 t_1(\Delta^e) \\ -2t_1(\Delta^e) & U \end{pmatrix}, \quad (\text{A2})$$

where

$$V(\Delta^e) = \frac{U}{\sqrt{1 + (Ur(\Delta^e)/14.397)^2}}, \quad (\text{A3})$$

$$r(\Delta^e) = r_0 - \Delta^e/2\alpha, \quad (\text{A4})$$

and

$$t_1(\Delta^e) = t_0 + \Delta^e/2. \quad (\text{A5})$$

The ground state energy is

$$\epsilon_0 = \frac{1}{2}([U + V(\Delta^e)] - \{[U - V(\Delta^e)]^2 + 16t_1(\Delta^e)^2\}^{1/2}), \quad (\text{A6})$$

with the eigenstate

$$|\Psi_0\rangle = \cos \theta |1\rangle + \sin \theta |2\rangle, \quad (\text{A7})$$

where

$$\theta = \tan^{-1}\left(\frac{V - \epsilon_0}{2t_1}\right). \quad (\text{A8})$$

Setting the bond force to zero gives

$$-\frac{\partial t_1(\Delta^e)}{\partial \Delta^e} \langle \hat{T} \rangle + \frac{\partial V(\Delta^e)}{\partial \Delta^e} \langle (\hat{n}_1 - 1)(\hat{n}_2 - 1) \rangle + \frac{\Delta^e}{2\pi t_0 \lambda} = 0. \quad (\text{A9})$$

Using Eq. (A7) to calculate the expectation value of the operators in Eq. (A9) leads to

$$\Delta^e = \frac{2\pi\alpha t_0 \lambda [\sin 2\theta - r_0 X(\Delta^e) \cos^2 \theta]}{\alpha - \pi t_0 \lambda X(\Delta^e) \cos^2 \theta}, \quad (\text{A10})$$

with

$$X(\Delta^e) = \frac{U\beta}{2\alpha[1 + \beta r(\Delta^e)^2]^{3/2}}. \quad (\text{A11})$$

This is a self-consistent equation for  $\Delta^e$ , which is solved iteratively.

\*Email address: W.Barford@sheffield.ac.uk

†Email address: ph1rb@phys.unsw.edu.au

<sup>1</sup>S. R. White, Phys. Rev. Lett. **69**, 2863 (1992); *Density Matrix Renormalization*, edited by I. Peschel, X. Wang, M. Kaulke, and K. Hallberg (Springer, Berlin, 1999).

<sup>2</sup>R. J. Bursill and W. Barford, Phys. Rev. Lett. **82**, 1514 (1999).

<sup>3</sup>W. Barford, R. J. Bursill, and M. Yu Lavrentiev, Phys. Rev. B **63**, 195108 (2001).

<sup>4</sup>B. E. Kohler and D. E. Schilke, J. Chem. Phys. **86**, 5214 (1987).

<sup>5</sup>P. Townsend, W.-S. Fann, S. Etemad, G. L. Baker, Z. G. Soos, and P. C. M. McWilliams, Chem. Phys. Lett. **180**, 485 (1991).

<sup>6</sup>A. Race, W. Barford, and R. J. Bursill, Phys. Rev. B **64**, 035208 (2001).

<sup>7</sup>R. Giesa and R. C. Schultz, Polym. Int. **33**, 43 (1994).

<sup>8</sup>L. Sebastian and G. Weiser, Phys. Rev. Lett. **46**, 1156 (1981); G. Weiser, Phys. Rev. B **45**, 14 076 (1992); A. Horvath, G. Weiser, C. Laperonne-Meyer, M. Schott, and S. Spagnoli, *ibid.* **53**, 13 507 (1996).

<sup>9</sup>S. Möller and G. Weiser, Chem. Phys. **246**, 483 (1999).

<sup>10</sup>More correctly, we should use the phrase “extrinsic tetramerization” rather than “extrinsic dimerization,” as there are four sites per unit cell.

<sup>11</sup>Our parametrization procedure is not quite consistent. We used a value of  $\alpha = 4.593 \text{ eV \AA}^{-1}$  in (Ref. 6) to determine the fixed-geometry hybridization integrals used in Ref. 6 with which we

parametrize  $\lambda$  in this paper. For a fixed spring constant  $K$ , this gives a new value of  $\alpha = 4.062 \text{ eV \AA}^{-1}$ . However, since the hybridization integrals themselves are only weakly dependent on  $\alpha$ , these differences in  $\alpha$  will cause changes in the hybridization integrals of only circa 0.01 eV.

<sup>12</sup>E. Ehrenfreund, Z. Vardeny, O. Barfman, and B. Horovitz, Phys. Rev. B **36**, 1535 (1987).

<sup>13</sup>*Conjugated Conducting Polymers*, edited by H. Kiess (Springer, Berlin, 1998), Chap. 2.

<sup>14</sup>H. Sixl, W. Neumann, R. Huber, V. Denner, and E. Sigmund, Phys. Rev. B **31**, 142 (1985).

<sup>15</sup>M.-H. Whangbo, R. Hoffman, and R. B. Woodward, Proc. R. Soc. London, Ser. A **366**, 23 (1979).

<sup>16</sup>M. Winter, A. Grupp, M. Mehring, and H. Sixl, Chem. Phys. Lett. **133**, 482 (1987).

<sup>17</sup>W. Barford, R. J. Bursill, and M. Yu Lavrentiev, Phys. Rev. B **65**, 075107 (2002).

<sup>18</sup>E. E. Moore and D. Yaron, J. Chem. Phys. **109**, 6147 (1998).

<sup>19</sup>F. Gebhard (private communication).

<sup>20</sup>P. Horsch, Phys. Rev. B **24**, 7351 (1981).

<sup>21</sup>G. König and G. Stollhoff, Phys. Rev. Lett. **65**, 1239 (1990).

<sup>22</sup>P. Tavan and K. Schulten Phys. Rev. B **36**, 4337 (1987).

<sup>23</sup>G. W. Hayden and E. J. Mele, Phys. Rev. B **34**, 5484 (1986).

<sup>24</sup>W. P. Su, Phys. Rev. Lett. **74**, 1167 (1995).

<sup>25</sup>K. Schulten and K. Karpus, Chem. Phys. Lett. **14**, 305 (1972).